A Numerical Method for Studying Impulsively Generated Convection from Heated Tubes

Serge D'Alessio
sdalessio@uwaterloo.ca

Department of Applied Mathematics
University of Waterloo
Waterloo, CANADA

CMEM 2007

Outline

University of Waterloo

Flow Configuration

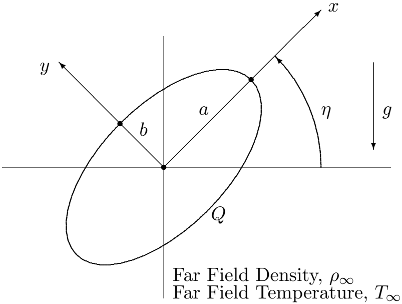

Far Field Density, ρ_∞
Far Field Temperature, T_∞

Fluid Properties:
ν - kinematic viscosity
κ - thermal diffusivity
k - thermal conductivity
α - thermal expansion coefficient
Equation of State:
$\rho = \rho_\infty[1 - \alpha(T - T_\infty)]$
Dimensionless Parameters:
$Gr = \dfrac{\alpha g \Delta T c^3}{\nu^2}$ where $c = \sqrt{a^2 - b^2}$
and $\Delta T = \dfrac{Qc}{k}$, $Pr = \dfrac{\nu}{\kappa}, \eta, r$

Applications

Unsteady free convection from a heated tube is a fundamental problem and is of interest for theoretical and practical reasons. Applications include:

- hot wire anemometry
- thermal pollution
- design of heat exchangers

Goals

The present study differs from previous investigations in the following ways:

- extend previous results on circular cylinders ([1])
- propose a new robust numerical method designed to capture the known physical behaviour
- offer an analytical solution procedure useful for theoretical and validation purposes

Coordinate System

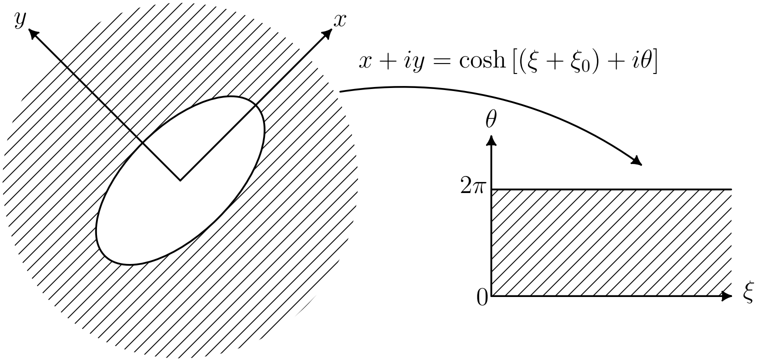

Navier-Stokes & Temperature Equations

The dimensionless unsteady equations for a viscous, incompressible fluid in terms of the streamfunction, ψ, vorticity, ζ, and temperature, ϕ, are:

$$\frac{\partial^2 \psi}{\partial \xi^2} + \frac{\partial^2 \psi}{\partial \theta^2} = M^2 \zeta$$

$$\frac{\partial \zeta}{\partial t} = \frac{1}{M^2}\left[\frac{\partial \psi}{\partial \theta}\frac{\partial \zeta}{\partial \xi} - \frac{\partial \psi}{\partial \xi}\frac{\partial \zeta}{\partial \theta} + \frac{1}{\sqrt{Gr}}\left(\frac{\partial^2 \zeta}{\partial \xi^2} + \frac{\partial^2 \zeta}{\partial \theta^2}\right) + A\frac{\partial \phi}{\partial \xi} - B\frac{\partial \phi}{\partial \theta}\right]$$

$$\frac{\partial \phi}{\partial t} = \frac{1}{M^2}\left[\frac{\partial \psi}{\partial \theta}\frac{\partial \phi}{\partial \xi} - \frac{\partial \psi}{\partial \xi}\frac{\partial \phi}{\partial \theta} + \frac{1}{\sqrt{Gr}\,Pr}\left(\frac{\partial^2 \phi}{\partial \xi^2} + \frac{\partial^2 \phi}{\partial \theta^2}\right)\right]$$

where functions M, A, B are related to the geometry.

Boundary, Initial & Integral Conditions

Surface conditions include no-slip and constant heat flux:

$$\psi = \frac{\partial \psi}{\partial \xi} = 0 \quad \text{and} \quad \frac{1}{M}\frac{\partial \phi}{\partial \xi} = -1 \quad \text{on} \quad \xi = 0$$

Far-field conditions: $\psi\ ,\ \zeta\ ,\ \phi \to 0\ \text{ as }\ \xi \to \infty$

Initial conditions: $\psi = \zeta = \phi = 0$ at $t = 0$

The vorticity can be shown to satisfy global conditions:

$$\int_0^\infty \int_0^{2\pi} e^{-n\xi} M^2 \zeta \sin(n\theta)\, d\theta\, d\xi = 0\ ,\ \ n = 1, 2, \cdots$$

$$\int_0^\infty \int_0^{2\pi} e^{-n\xi} M^2 \zeta \cos(n\theta)\, d\theta\, d\xi = 0\ ,\ \ n = 0, 1, \cdots$$

Boundary Layer Transformation

Introduce boundary-layer coordinate: $\xi = \lambda z \ , \ \lambda = \sqrt{\frac{4t}{\sqrt{Gr}}}$

The grid expands with time as illustrated below:

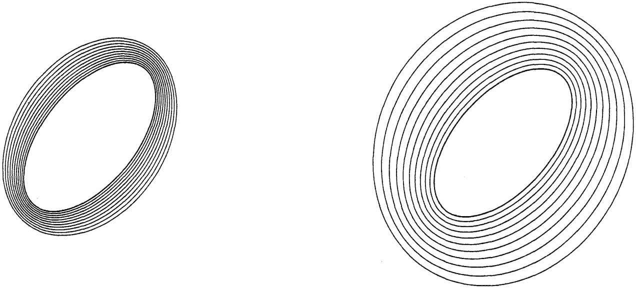

Boundary Layer Transformation

The governing equations then become:

$$\frac{\partial^2\psi}{\partial z^2} + \lambda^2 \frac{\partial^2\psi}{\partial\theta^2} = \lambda^2 M^2 \zeta$$

$$\frac{1}{M^2}\frac{\partial^2\zeta}{\partial z^2} + 2z\frac{\partial\zeta}{\partial z} = 4t\frac{\partial\zeta}{\partial t} - \frac{\lambda^2}{M^2}\frac{\partial^2\zeta}{\partial\theta^2}$$
$$+\frac{4t}{\lambda M^2}\left(\frac{\partial\psi}{\partial z}\frac{\partial\zeta}{\partial\theta} - \frac{\partial\psi}{\partial\theta}\frac{\partial\zeta}{\partial z}\right) - \frac{4tA}{\lambda M^2}\frac{\partial\phi}{\partial z} + \frac{4tB}{M^2}\frac{\partial\phi}{\partial\theta}$$

$$\frac{1}{PrM^2}\frac{\partial^2\phi}{\partial z^2} + 2z\frac{\partial\phi}{\partial z} = 4t\frac{\partial\phi}{\partial t} - \frac{\lambda^2}{PrM^2}\frac{\partial^2\phi}{\partial\theta^2} + \frac{4t}{\lambda M^2}\left(\frac{\partial\psi}{\partial z}\frac{\partial\phi}{\partial\theta} - \frac{\partial\psi}{\partial\theta}\frac{\partial\phi}{\partial z}\right)$$

Discretization

Early stages of the flow are computed using the boundary-layer coordinate z. Once the boundary layer thickens the flow is computed using the original coordinate ξ. For large Gr it is more practical to work entirely in the coordinate z.

The computational domain bounded by $0 \leq z \leq z_\infty$ and $0 \leq \theta \leq 2\pi$ is discretized into a uniform network of $K \times L$ grid points located at

$$z_i = ih_z \ , \ i = 0, 1, \dots, K \ , \ h_z = \frac{z_\infty}{K}$$

$$\theta_j = jh_\theta \ , \ j = 0, 1, \dots, L \ , \ h_\theta = \frac{2\pi}{L}$$

z_∞ denotes the outer boundary approximating infinity.

Solution of Streamfunction

The streamfunction is expanded into a truncated Fourier series

$$\psi(z,\theta,t) = \frac{1}{2}F_0(z,t) + \sum_{n=1}^{N}[F_n(z,t)\cos(n\theta) + f_n(z,t)\sin(n\theta)]$$

The Fourier coefficients satisfy

$$\frac{\partial^2 F_n}{\partial z^2} - n^2\lambda^2 F_n = \lambda^2 s_n(z,t)\ ,\ \ n = 0,\ 1,\ \cdots$$

$$\frac{\partial^2 f_n}{\partial z^2} - n^2\lambda^2 f_n = \lambda^2 r_n(z,t)\ ,\ \ n = 1,\ \cdots$$

At a fixed time these equations are effectively ODEs and are integrated using marching algorithms.

Solution of Streamfunction

The functions $r_n(z,t)$ and $s_n(z,t)$ are given by

$$s_n(z,t) = \frac{1}{\pi}\int_0^{2\pi} M^2\zeta\cos(n\theta)d\theta$$

$$r_n(z,t) = \frac{1}{\pi}\int_0^{2\pi} M^2\zeta\sin(n\theta)d\theta$$

and satisfy the intergal conditions

$$\int_0^{\infty} \mathrm{e}^{-n\lambda z} s_n(z,t)dz = 0 \ , \ \ n = 0,1,2,\cdots$$

$$\int_0^{\infty} \mathrm{e}^{-n\lambda z} r_n(z,t)dz = 0 \ , \ \ n = 1,2,\cdots$$

Solution of Vorticity & Temperature

The transport equations for ζ, ϕ can be cast in generic form

$$t\frac{\partial \chi}{\partial t} = q(z, \theta, t)$$

This equation is solved using the Crank-Nicholson implicit procedure. The solution is advanced from time t to time $t + \Delta t$ by integrating the above

$$\chi\tau|_t^{t+\Delta t} - \int_t^{t+\Delta t} \chi d\tau = \int_t^{t+\Delta t} q d\tau$$

Approximating the integrals using the trapezoidal rule yields

$$\chi(z, \theta, t + \Delta t) = \chi(z, \theta, t) + (\frac{\Delta t}{2t + \Delta t})[q(z, \theta, t + \Delta t) + q(z, \theta, t)]$$

The resulting algebraic system is then solved iteratively.

Determination of Surface Vorticity

The surface vorticity is determined by inverting the expressions for r_n and s_n. This leads to the truncated Fourier series

$$\zeta(0,\theta,t) = \frac{1}{M_0^2}\{\frac{1}{2}s_0(0,t)+\sum_{n=1}^{N}[r_n(0,t)\sin(n\theta)+s_n(0,t)\cos(n\theta)]\}$$

The quantities $s_n(0,t)$ and $r_n(0,t)$ are computed by enforcing the integral conditions. That is, off the cylinder surface r_n and s_n can be computed using the most recent guess for ζ. Then, $s_n(0,t)$ and $r_n(0,t)$ are computed by numerically satisfying the integral constraints.

Summary of Numerical Algorithm

The following steps are performed ($p \equiv$ iteration counter):

1. solve for $\phi^{(p)}(z, \theta, t + \Delta t)$,
2. solve for $\zeta^{(p)}(z, \theta, t + \Delta t)$ for $z \neq 0$,
3. compute $r_n^{(p)}(z, t + \Delta t)$, $s_n^{(p)}(z, t + \Delta t)$ for $z \neq 0$,
4. calculate $r_n^{(p)}(0, t + \Delta t)$, $s_n^{(p)}(0, t + \Delta t)$ by enforcing the integral conditions and hence compute $\zeta^{(p)}(0, \theta, t + \Delta t)$,
5. solve for $f_n^{(p)}(z, t + \Delta t)$, $F_n^{(p)}(z, t + \Delta t)$ and thus obtain $\psi^{(p)}(z, \theta, t + \Delta t)$,
6. repeat above steps till convergence is reached and increment p by 1.

Convergence is reached when the difference between two successive iterates of the surface vorticity is less than ϵ.

Computational Parameters

After performing numerous numerical experiments, the following computational parameters were chosen:

$$N = 25 \ , \ \epsilon = 10^{-6} \ , \ z_{\infty} = 10$$

A typical grid size used was $K \times L = 200 \times 120$. Because of the impulsive start, small time steps of $\Delta t = 10^{-3}$ were used initially. As time increased the time step was gradually increased to $\Delta t = 0.05$. Results were obtained using values

$$r = 0.5 \ , \ \eta = 45^{\circ} \ , \ Pr = 0.7 \ \text{ for } \ Gr = 10^2 \ \text{ and } \ Gr = 10^4$$

Isotherm Plots

Isotherm plot for $Gr = 10^2, \eta = \frac{\pi}{4}$, $Pr = 0.7, r = 0.5$ at $t = 2.5$ (conduction regime).

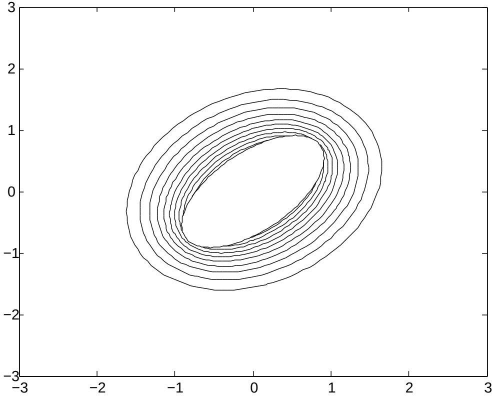

Isotherm Plots

Isotherm plot for $Gr = 10^2, \eta = \frac{\pi}{4}$, $Pr = 0.7, r = 0.5$ at $t = 100$ (well developed plume).

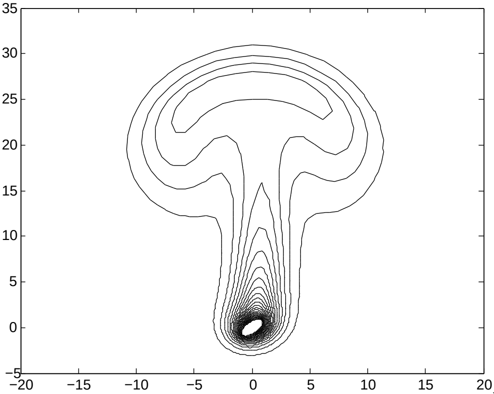

Isotherm Plots

Isotherm plot for $Gr = 10^4, \eta = \frac{\pi}{4}$, $Pr = 0.7, r = 0.5$ at $t = 15$.

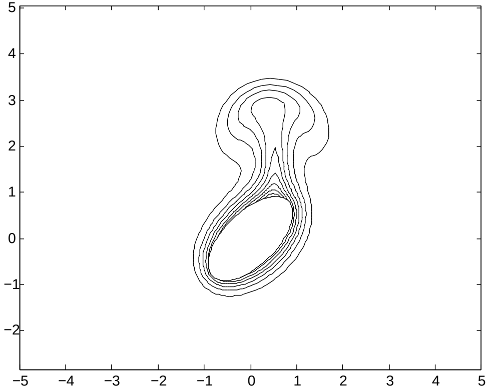

Isotherm Plots

Isotherm plot for $Gr = 10^4, \eta = \frac{\pi}{4}$, $Pr = 0.7, r = 0.5$ at $t = 20$.

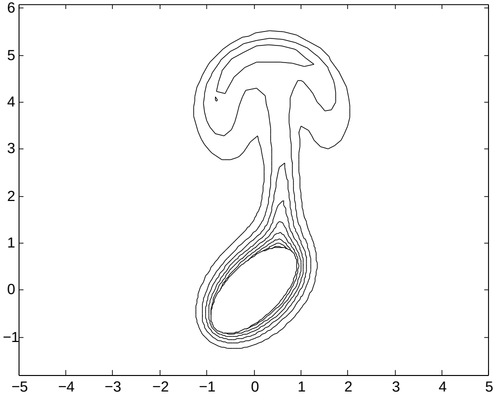

Isotherm Plots

Isotherm plot for $Gr = 10^4, \eta = \frac{\pi}{4}$, $Pr = 0.7, r = 0.5$ at $t = 25$.

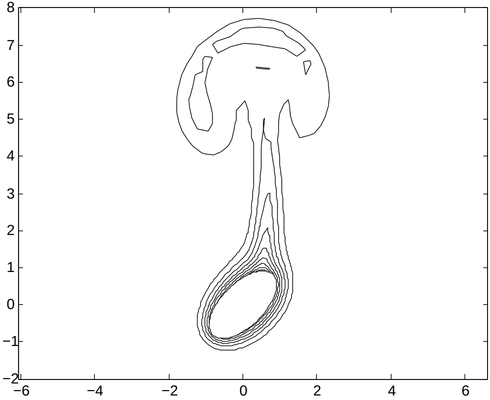

Surface Vorticity Plots

Surface vorticity distributions for $Gr = 10^4, \eta = \frac{\pi}{4}$, $Pr = 0.7, r = 0.5$.

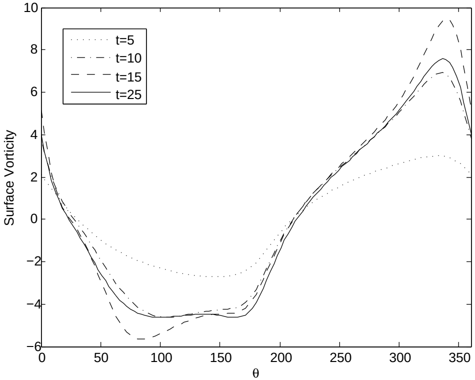

Surface Temperature Plots

Surface temperature distributions for $Gr = 10^4, \eta = \frac{\pi}{4}$, $Pr = 0.7, r = 0.5$.

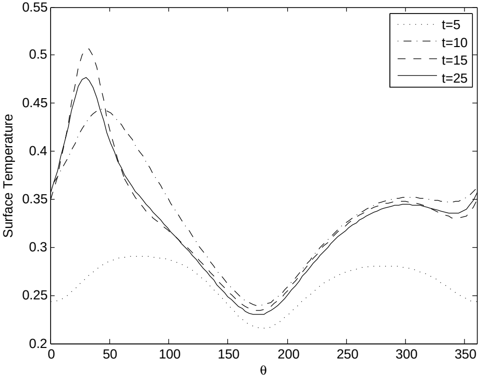

Analytical Validation

For large *Gr* and small *t* it is possible to expand the flow variables in the double series:

$$\chi = \chi_0 + \lambda\chi_1 + \lambda^2\chi_2 + \cdots$$

where each χ_n $(n = 0, 1, 2, \cdots)$ is further expanded:

$$\chi_n(z,\theta,t) = \chi_{n0}(z,\theta) + t\chi_{n1}(z,\theta) + \cdots$$

The leading-order solution for the temperature is:

$$\phi(z,\theta,t) \sim \frac{2\sqrt{t}}{\sqrt{\pi Pr\sqrt{Gr}}}(e^{-PrM_0^2z^2} - \sqrt{\pi Pr}M_0 z\text{erfc}(\sqrt{Pr}M_0 z))$$

Average Surface Temperature

Comparison of time variation of average surface temperature for $Gr = 10^4, \eta = \frac{\pi}{4}, Pr = 0.7, r = 0.5$. Good agreement for small t; agreement worsens with time.

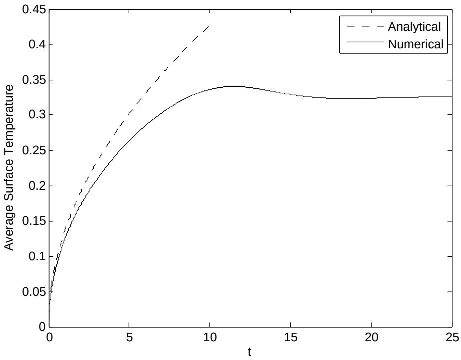

Concluding Remarks

- Impulsively generated convection from an elliptic cylinder was investigated
- The numerical method presented is successful for computing unsteady flows for a wide range of Grashof numbers
- Numerical results were supported by analytical results
- The technique can be easily extended to handle other cross sections
- Future work includes comparisons with experiments ([4])